

Adiabatic Compression of Soliton Matter Waves

F. Kh. Abdullaev† and Mario Salerno ‡

†Physical-Technical Institute, Uzbek Academy of Sciences, 2-b, Mavlyanov str.,
700084 Tashkent, Uzbekistan.

‡Dipartimento di Fisica "E.R. Caianiello", Università di Salerno, I-84081 Baronissi
(SA), Italy, and Istituto Nazionale di Fisica della Materia (INFN), Unità di Salerno,
Italy.

E-mail: fatkh@physic.uzsci.net, salerno@sa.infn.it

Abstract. The evolution of atomic solitary waves in Bose-Einstein condensate (BEC) under adiabatic changes of the atomic scattering length is investigated. The variations of amplitude, width, and velocity of soliton are found for both spatial and time adiabatic variations. The possibility to use these variations to compress solitons up to very high local matter densities is shown both in absence and in presence of a parabolic confining potential.

PACS numbers: 03.75.Fi, 03.75.-b, 05.45.Yv

Submitted to: *J. Phys. B: At. Mol. Phys.*

1. Introduction

The discovery of Bose-Einstein condensates (BEC) in atomic vapors of alkali metals has opened new possibilities to observe matter waves of soliton type. These excitations were first discovered in BEC with repulsive interatomic interactions, in the form of dark solitons [1], and more recently, in BEC with attractive interatomic interactions, in the form of bright solitons moving on zero backgrounds [2, 3]. Since soliton matter waves are of primary importance for developing concrete applications, it is of interest to devise methods which allow to control them. One possibility is to vary the atomic scattering length by means of external magnetic fields, i.e. by using Feshbach resonances. In Ref. [4], it was shown that an abrupt change in time of the atomic scattering length, can lead to the splitting of the soliton with the generation of new solitons. The fragmentation of the wave obviously decreases the number of atoms contained in the original pulse, this being undesirable for applications such as atom lasers.

In the present paper we suggest to use *adiabatic* variations of the atomic scattering length, both in time and in space, as an effective way for controlling soliton's parameters and to induce changes in their shape which could be useful for applications. In contrast to abrupt variations, adiabatic changes make possible to preserve the integrity of the

soliton (no splitting occurs), this leading for bright solitons to the compression of the pulse with the increase of the matter density, and for dark solitons to the compression of the hole with a decrease of the background level (matter from background move inside the hole). These phenomena are shown to exist both in presence and in absence of a parabolic confining potential. In the last case we derive analytical equations for soliton parameters in terms of adiabatic invariants and soliton perturbation theory. The results of this analysis is found in good agreement with direct integration of the 1D Gross-Pitaevskii equation (GPE). The effect of a confining parabolic potential on the adiabatic dynamics of the soliton is also investigated by numerical simulations. We find that, for bright solitons, except for the oscillatory motion around the bottom of the trap, the phenomena of pulse compression is practically the same as in absence of the trap (this is particularly true for solitons initially at rest in the bottom of the trap). For dark soliton the phenomenon is only qualitatively preserved, due to the boundaries effects introduced by the trap. The possibility to compress BEC solitons could be an experimental tool to investigate the range of validity of the 1D GPE. Since the quasi one dimensional regime is valid for low densities, it would be indeed interesting to see how far one can compress a soliton in a real experiment by means of adiabatic changes of the scattering length. Effects of adiabatic perturbations on soliton dynamics were also investigated in the context of Josephson junctions [5] and in nonlinear optics [6]. In contrast with Josephson junctions and optical fibers, which require structural changes or preparation of new samples, the study of adiabatic nonlinear perturbations on BEC solitons appears more natural and easy to perform, since the strength of the nonlinear interaction can be changed by using only external fields. We also remark that soliton dynamics in a quasi one-dimensional BEC under time-dependent *linear* potential was recently studied in [7].

The paper is organized as follows. In Section 1 we perform an analytical study of the effects on bright and dark BEC solitons induced by spatial and temporal adiabatic variations of the scattering length. For temporal variations we use both a variational approach and perturbation theory to obtain equations for soliton's parameters both in presence and absence of a confining parabolic potential. In the former case the problem can be linked to an adiabatic invariant of the Kepler problem with results depending only on adiabaticity (smoothness) but not on the smallness of the perturbation. For spatial variations we use standard soliton's perturbation theory. In Section 2 we compare the results of this analysis with direct numerical integrations of the full 1D GPE both in absence and in presence of an harmonic trap. In the last section we summarize the main results of the paper.

2. Analysis

The dynamics of a dilute trapped BEC is described by the Gross-Pitaevskii equation (GPE)

$$i\hbar\phi_t(r, t) = -\frac{\hbar^2}{2m}\Delta\phi(r, t) + V_{tr}(r, t)\phi(r, t) + \Gamma|\phi|^2\phi(r, t), \quad (1)$$

with $\Gamma = \frac{4\pi\hbar^2 a_s}{m}$, m being the atomic mass, a_s the scattering length, and $V_{tr} = \frac{1}{2}m(\omega_1^2 x^2 + \omega_2^2 y^2 + \omega_3^2 z^2)$ represents the harmonic trap. The quasi 1D geometry corresponds to the case $\omega_1^2 \ll \omega_{2,3}^2$. To model adiabatic variation of the atomic scattering in 1D (cigar shaped) BEC we consider the following normalized Gross-Pitaevskii equation [8, 9]

$$i\psi_t + \psi_{xx} + \sigma\gamma(x, t)\psi|\psi|^2 - \omega^2 x^2\psi = 0, \quad (2)$$

where ψ is the ground state wavefunction of the condensate, $\gamma(x, t)$ is a slowly varying function of space and time, $\sigma \pm 1$ corresponds to the case of negative and positive scattering length a_s (ω denotes the longitudinal frequency of the trap). In Eq. (2) the space has been normalized with respect to the healing length $\xi = 1/\sqrt{8\pi\rho|a_s|}$ (ρ is the atomic density), while the time with respect to $t_0 = m\xi^2/\hbar$. We remark that the 1D approximation is valid for the number of atoms $N < l_r/|a_s|$, where $l_r = \sqrt{\hbar/(m\omega_{2,3})}$ is the transverse oscillator length. It is also worth to mention that in the strong interaction limit $a_s N |\psi|^2 \gg 1$, ($a_s > 0$), the effective nonlinearity is of the type $|\psi|\psi$ [13] so that deviations from Eq. (2) occur (this will not be considered in this paper). Although the analysis can be performed for a generic smooth functions $\gamma(x, t)$, we shall restrict to the limiting cases: $\gamma \equiv \gamma(t)$, and $\gamma \equiv \gamma(x)$, the former being experimentally more easy to realize.

2.1. Case $\gamma \equiv \gamma(t)$

To study adiabatic temporal variations of the scattering length, *case* $\gamma \equiv \gamma(t)$, we remark that, due to the number of atoms conservation, it is natural to look for solution of Eq. (2) with $\sigma = +1$ (negative scattering length) in the form of a bright soliton with time dependent parameters

$$\psi(x, t) = A(t)\text{sech}\left(\frac{x - \zeta(t)}{a(t)}\right)e^{ib(t)(x - \zeta(t))^2 + iC(x - \zeta(t)) + i\phi(t)}, \quad (3)$$

where $A(t)$, $a(t)$, $\phi(t)$, $\zeta(t)$, $C(t)$, $b(t)$, denote, respectively, amplitude, width, phase, center, velocity and "chirp" oscillation of the perturbed soliton. Taking these parameters (with their derivatives), as collective coordinates for the soliton, one can derive their time evolution from the Euler-Lagrange equations with respect to the space averaged Lagrangian $\bar{L} = \int L(x, t)dx$ of Eq. (2) [10]. This gives for the center of mass: $\zeta_{tt} + 4\omega^2\zeta = 0$, and for the width [11]:

$$a_{tt} + 4\omega^2 a = \frac{16}{\pi^2 a^3} - \frac{4\gamma(t)N}{\pi^2 a^2}. \quad (4)$$

Notice that Eq. (4) has the form of a perturbed Kepler problem [12]. This analogy can be used to reformulate the problem in terms of the evolution of a unit mass moving in an

adiabatically varying Kepler potential. Since action-angle variables for the unperturbed case are known, one can describe the adiabatic change of the soliton width by means of the adiabatic invariant of the Kepler problem. As the result we find for $\omega^2 < 1$ that

$$a \approx \frac{4}{\gamma(t)N} \left[1 - \frac{64\omega^2}{(\gamma(t)N)^4} \right]. \quad (5)$$

We see that for $\omega = 0$ one recovers the law $a = 4/(\gamma(t)N)$ known from nonlinear fiber optics. In this case, one can also show that the frequency of the width oscillation is given by $\omega_a \approx \gamma^2(t)N^2/4\pi$. The analysis can be easily extended to two dimensions (2D) for the radially symmetric GPE. In this case the variational equation for the width becomes $a_{tt} + 2\omega^2 a = \frac{2(2-N_1\gamma_1(t))}{a^3}$, where $N_1 = N/(2\pi)$, $\gamma_1 = \gamma/(\sqrt{2}\pi l_x)$. Applying the above arguments, one finds that the width of a 2D soliton changes as $a \approx (2 - N_1\gamma_1(t))^{1/4}/\omega^{1/2}$. Eq. (5) predicts for small ω a dependence $1/\gamma$ of the soliton width. This result can also be obtained by perturbation theory. To this end we assume in the following that the range of variation of the potential is very large in comparison with the size of the condensate, so that we can neglect the ω term in Eq. (2) (this is particularly appropriate for static bright solitons located at the bottom of the trap, as we will show later). In this case the transformation $\psi = u/\sqrt{\gamma}$ (for $\gamma > 0$), allows to rewrite Eq. (2) in the form of a perturbed nonlinear Schrödinger equation

$$iu_t + u_{xx} + |u|^2 u = i(\ln \sqrt{\gamma})_t u + (\ln(\gamma))_x u_x + 0\left(\frac{T^2}{T^2}, \frac{L^2}{L^2}\right) = R(u), \quad (6)$$

where T and L are, respectively, the temporal and spatial characteristic scales of the inhomogeneity, while T_s, L_s are characteristic time and space soliton scales, assumed to be much smaller than the corresponding inhomogeneity scales. In the case $\gamma_x = 0$, the right hand side of Eq. (6) represents a small linear time dependent amplification (damping). If we consider the initial condition as a single soliton

$$u(x, t) = \sqrt{2}A(t)\text{sech}(A(t)(x - \zeta))e^{i\Theta(t)}, \quad \Theta = k(t) + C(t)(x - \zeta(t)), \quad (7)$$

then, using the equation for the energy $N = \int |u|^2 dx$, we find $A = A_0\gamma(t)$ this giving, for the amplitude and width of the soliton, $A_\psi = A_0\sqrt{\gamma}$, $a = 1/(A_0\gamma)$, in agreement with the variational approach. From this we conclude that an adiabatic increase of the scattering length can be used to narrowing the width of a bright soliton matter wave. Soliton compression phenomena induced by linear damping amplification are also known from nonlinear optics [6, 12]. A similar analysis can be performed for the adiabatic evolution of a dark soliton ($\sigma = -1$ in Eq.(2)). In this case, the adiabatic evolution of the dark soliton ψ_d and of the background u_B can be found as

$$\psi_d = u_0 \tanh\left(\frac{u_0\sqrt{\gamma}}{\sqrt{2}}(x)\right)e^{-i\theta}, \quad u_B = u_0\sqrt{\gamma} \exp(-i\theta), \quad \theta = -iu_0^2 \int_0^t \gamma(t') dt', \quad (8)$$

where $u_0 = \sqrt{\mu}$, with μ the chemical potential of the condensate (notice that this last expression for u_B is exact). From this expression we see that the width of the dark soliton is changing according to $a_d = a_{d0}/\sqrt{\gamma(t)}$, i.e. a factor $1/\sqrt{\gamma(t)}$ less in comparison with bright solitons.

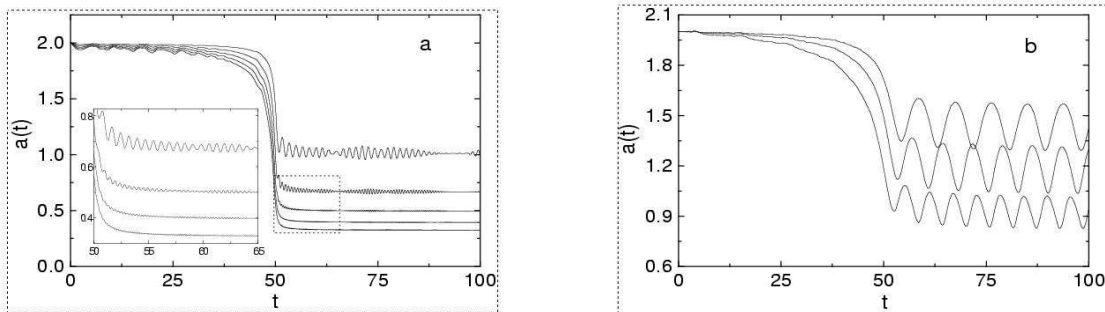


Figure 1. a) Soliton's width vs. time for different values of A_s . Panel a) refers to the bright soliton case ($\sigma = 1$) The values of A_s are stepped by 2, from $A_s = 2$ (top curve) to $A_s = 10$ (bottom curve). The other parameters are $s = 0.5, T_f = 100, \sigma = 1, v_s = 0$. An enlargement of the broken line box, showing rapidly decreasing oscillations for increasing A_s values, is reported in the inset. Panel b) refers to the dark soliton case ($\sigma = -1$ for A_s values 2, 4, 8, (from top to bottom). The other parameters are $s = 0.1, T_f = 100, v_s = 0$.

2.2. Case $\gamma \equiv \gamma(x)$

The perturbative approach can be used to study also the case of spatial variations of the scattering length *i.e.* $\gamma \equiv \gamma(x)$. We have from Eq. (6): $R(u) = F(x)u_x$, $F = (\ln \gamma(x))_x$, with $R(u)$ considered to be a small perturbation. Using the perturbation theory for solitons [14], we find that the equations for the soliton's parameters (7) are:

$$\begin{aligned} A_t &= AC \int_{-\infty}^{\infty} F\left(\frac{y}{A} + \zeta\right) \text{sech}^2(y) dy \approx 2ACF(\zeta), \\ C_t &= A^2 \int_{-\infty}^{\infty} F\left(\frac{y}{A} + \zeta\right) (\text{sech}^2(y) - \text{sech}^4(y)) dy \approx \frac{2}{3}A^2F(\zeta), \\ \zeta_t &= 2C + \frac{C}{A} \int_{-\infty}^{\infty} F\left(\frac{y}{A} + \zeta\right) y \text{sech}^2(y) dy \approx 2C(1 + O(\frac{1}{L^2})). \end{aligned} \quad (9)$$

From these equations it follows that ($F(-\infty) = 1$)

$$A = A_0\gamma(\zeta), C_{fin} = \sqrt{C_{in}^2 + \frac{1}{3}A_0^2(\gamma^2(\zeta) - \gamma_{ini}^2)}. \quad (10)$$

In the next section we shall compare these predictions with direct numerical integrations of Eq.(2).

3. Numerical results

To check these results we have numerically integrated Eq. (2) with the function $\gamma(t)$ given by

$$\gamma(t) = 2 + A_s \left[\frac{1}{2} + \frac{1}{\pi} \tan^{-1}(s\pi)\left(t - \frac{T_f}{2}\right) \right] \quad (11)$$

This function models, for small s , an adiabatic change of the scattering length, while for large s it reduces to the step function of amplitude A_s centered at $T_f/2$ (to have

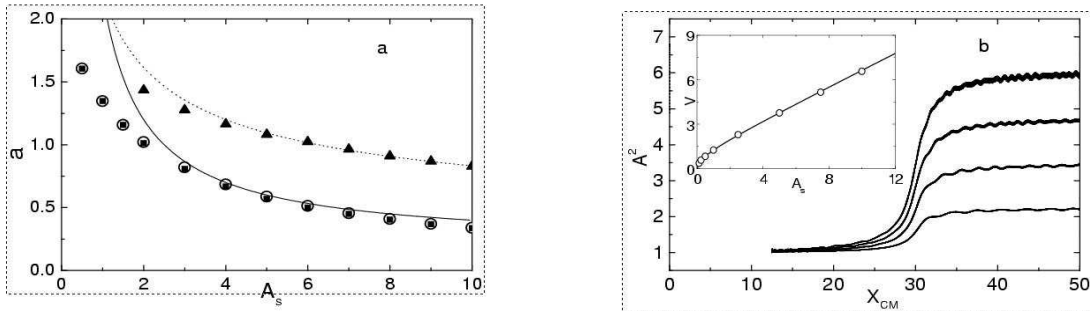


Figure 2. Panel a) Bright and dark soliton width versus step amplitude A_s , for parameter values $s = 0.1, T_f = 100$, and soliton velocity $v_s = 0$. The triangles and squares denote numerical values in absence of trap potential for $\sigma = 1$ (bright case) and $\sigma = -1$ (dark case), respectively. The open circles denote numerical values for the bright case in presence of a trap potential of frequency $\omega^2 = 0.01$ (the soliton is taken at rest in the bottom of the trap). The continuous and dashed curves are the analytical predictions in absence of trap potential for, respectively, bright and dark soliton case. Panel b) The squared amplitude of a bright soliton vs center of mass position for different values of the amplitude A_s of a kink-like spatial inhomogeneity centered at $x=30$, given by Eq. (11). The curves, from bottom to top, refer to $A_s = 2.5, 5.0, 7.5, 10.0$, respectively. The other parameters are $s = 0.2, T_f = 60, \sigma = 1, A_0 = 1$. The soliton is initially at rest, placed at position $x_{ini} = 12.5$. In the inset we show the soliton final velocity as a function of A_s . The open dots are numerical values while the continuous curve is obtained from Eqs. (10,10) as
$$V_{fin} = \frac{A_0}{\sqrt{3}} \sqrt{\gamma_{fin}^2 - \gamma_{in}^2}.$$

the function starting from 2, the quantity $\delta = \gamma(0) - 2$ must be subtracted). In the following we shall use this function to model also spatial variations of the scattering length. In Fig. 1 we depict the width of a bright (panel a) and a dark soliton (panel b) as a function of time for different values of A_s , in the case $\omega = 0$. From this figure we see that the oscillations of the soliton width after the transition, are more pronounced for dark solitons than for bright ones. This is a consequence of the fact that in the dark case the background is also excited by the perturbation and contribute for a relevant part to the dynamics. In Fig. 2a we show the average final value of the width of bright and dark solitons as a function of A_s . It is evident that, for the same absolute variation of the scattering length, bright solitons are more compressed than dark ones, the difference being just a factor proportional to $1/\sqrt{\gamma}$, as expected from our analysis. The agreement with the theoretical predictions is indeed rather good especially for higher values of A_s . Notice that in this figure the influence of a parabolic trap on the compression phenomenon is also shown for the case of a bright soliton initially at rest in the bottom of the trap (open circles). We see that the results are almost identical to those in absence of trap (this is quite expected, since the pulse is localized in the bottom of a low intensity trap). The panel (b) of the same figure shows the amplitude of a bright soliton as a function of the position of the center of mass for the case of a space dependent variation

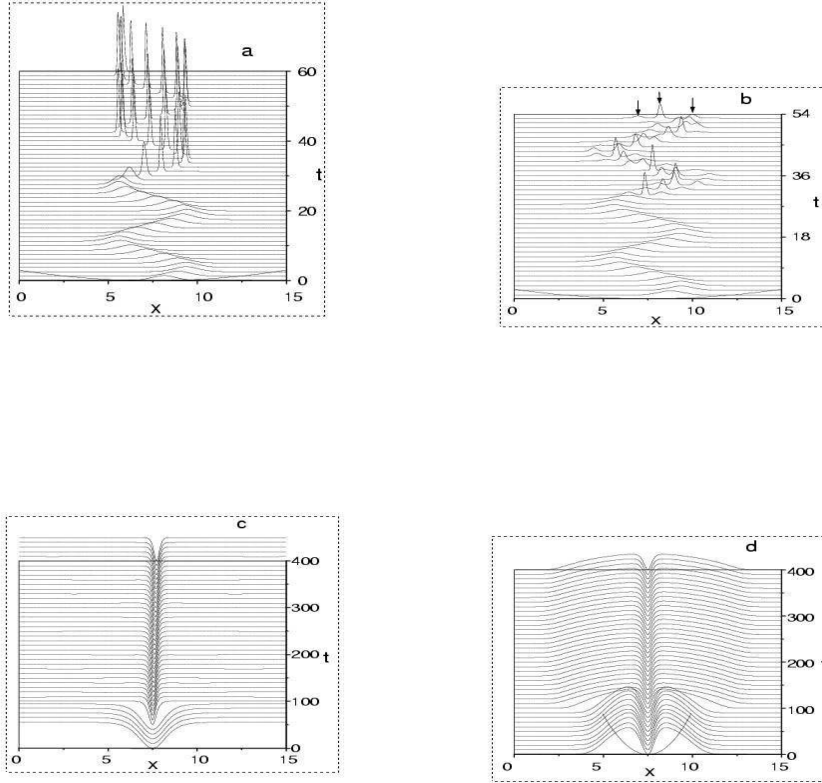


Figure 3. Time evolution of bright and dark solitons in absence and in presence of parabolic trap. Panels (a,b): Bright soliton dynamics ($\sigma = 1$) in presence of parabolic potential of frequency $\omega^2 = 0.04$ subject to (a) an adiabatic change $\gamma(t)$ of the scattering length with $A_s = 25$, $s = 0.5$, and $T_f = 50$; (b) a step like variation $\gamma(t)$ with $s = 10^4$. Other parameters are fixed as in panel (a). Panels (c,d): Dark soliton dynamics $\sigma = -1$ in absence (c) and in presence (d) of a parabolic trap of intensity $\omega^2 = 0.8$. In both cases the initial dark profiles are at rest and subject to a $\gamma(t)$ variation with parameters $A_s = 10$, $s = 0.5$, and $T_f = 200$. Notice that the parabolic potential is also shown at $t = 0$ to display the scale in the z -direction.

of the scattering length in absence of the parabolic trap. The soliton, is initially at rest, is sucked into the higher scattering length region, and reaches a constant velocity after passing the inhomogeneity. Also in this case we find an excellent agreement with our analysis (see the inset of the figure).

The effect of the parabolic trap on pulse compression is further investigated in Fig. 3. In panels (a) and (b) of this figure, we show the evolution of a bright soliton oscillating in the trap and subject, respectively, to adiabatic and abrupt variation of the scattering length. We see that in contrast with the adiabatic case, which always leads to compression, abrupt variations of the scattering length may induce the splitting of

the soliton into sub-solitons (notice in panel (b), that three solitons, indicated by the arrows, are formed at time $t = 54$). The splitting phenomenon is similar to the one observed in absence of parabolic potential [4]. The number of sub-solitons created can also be determined in analogy with this last case (we omit details for brevity). Panels (c) and (d) of Fig. 3, show the time evolution of a dark soliton in absence and in presence of a parabolic trap. We remark that, while in the bright case the compression of the soliton is obviously accompanied by an increase of its amplitude, in the dark case the amplitude cannot decrease below zero, so that the compression must be combined with a decrease of the background level (the matter from the background move inside the hole so to reduce its size). This is particularly evident in panel c for the case $\omega = 0$. We remark that this case, although physically non realisable for BEC, it is of interest for nonlinear optics, and shows the role played by the confinement potential in the case of BEC with positive scattering lengths (it should be compared with panel(d) discussed below).

In analogy with bright solitons, one could expect that an abrupt change in time of the scattering length may split a dark soliton ground state into dark and grey sub-components if the amplitude of the perturbation is big enough. This is indeed what we numerically observed. For the case $\omega = 0$, using the Inverse Scattering Transform, one can predict that out of an initial profile of the form $\psi(x, t = 0) = b \tanh(cx)$, one black soliton and a number N_0 of pairs of grey solitons (with $N_0 = n - 1$, n being the integer part of the ratio b/c) [15, 16], should be generated. By denoting with γ_1 and γ_2 the initial and final values of γ , one can write the initial condition for the equation: $iv_t + v_{xx} - |v|^2v = 0$, as $v(0) = u_0\sqrt{\gamma_2}\tanh(u_0\sqrt{2\gamma_1}x)$, with $v = \psi\sqrt{\gamma_2}$, and the ratio b/c equal to $\sqrt{\gamma_2/2\gamma_1}$. We checked that this analysis indeed gives correct predictions of splitting in absence of the parabolic trap. The influence of the parabolic trap on a dark soliton initially at the rest in its bottom, is reported in panel (d) of Fig. 3. Although the phenomenon resemble the one observed in absence of the trap (notice the decrease of the background after the transition), the solution is more complicated due to the boundary effects introduced by the trap. In particular we see that the compression of the hole in the center is less effective than for $\omega = 0$, and the decrease of the background is accompanied by an expansion of the condensate. This is a consequence of the non constancy of the background (it obviously must go to zero at large distances) which permits the matter to escape up in the trap (the pressure on the hole is thus partially lost in the expansion). The same phenomenon exists also for dark solitons initially oscillating in the trap. In analogy with the case $\omega = 0$, we also found that abrupt variations in presence of parabolic potential induce dark soliton splitting.

In Fig. 4 we show the averaged amplitude of the soliton (i.e. the time average of the modulo squared at the center of the profile) versus the parameter s controlling the rapidity of change of the function $\gamma(t)$. From this figure we see that a crossover from adiabatic to fast variations behavior occurs at $s \approx 1.2$. Notice that this crossover value of s corresponds to a variation function $\gamma(t)$ which is already quite rapid (see top inset of the figure). The adiabatic region is characterized by the fact that the final profiles of the

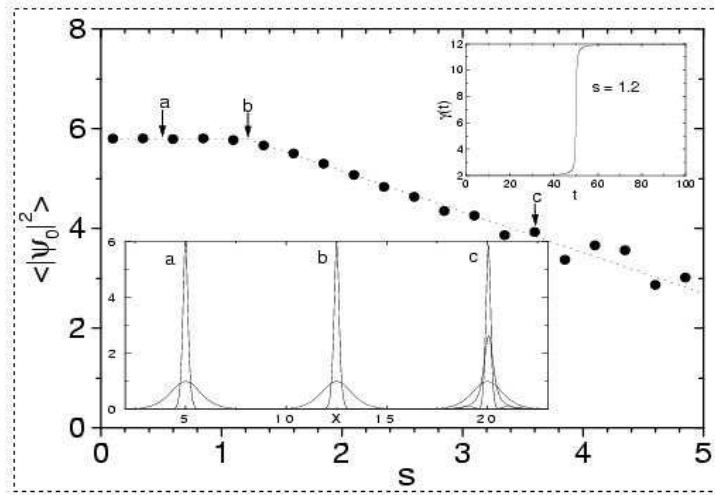


Figure 4. Time averaged amplitude of the soliton versus the parameter s of the scattering length function $\gamma(t)$. The amplitude and the time of the variation are fixed as $A_s = 10$ and $T_f = 100$. Notice the crossover from adiabatic to abrupt behavior occurring at $s \approx 1.2$ (dotted lines are drawn to guide the eyes). The inset at the top shows the shape of the function $\gamma(t)$ at the crossover point (point b). The inset at the bottom shows the initial and final profiles of the soliton at the points a, b, c , corresponding, respectively, to the values, $s = 0.5$, $s = 1.2$, $s = 3.6$. Soliton profiles corresponding to points a and c have been shifted by ± 7.5 along the x axis to avoid overlapping with the ones corresponding to point b.

compressed solitons are almost independent on s (they depend only on the amplitude of the scattering length variation). This can be seen from the bottom inset of Fig. 4 in which the initial ($t = 0$) and final ($t = 100$) soliton profiles corresponding to points a and b in the adiabatic region, are reported. Very little oscillations of the soliton profile are found in these cases. On the contrary, the non-adiabatic (or fast oscillation) region is characterized by the presence of large oscillations of the soliton profile, induced by the rapid variation of the scattering length. This is illustrated in point c of the lower inset of Fig. 4, in which we depicted, besides the initial profile at $t = 0$, two snapshots of the soliton (max and min of the profile) to evidenciate its oscillations at the final time $T_f = 100$. These oscillations increase by increasing s and eventually lead to the splitting of the soliton as illustrated in panel b of Fig. 3 (the splitting, however, depends also on the amplitude of the scattering length variation, and usually occurs much above the interface between adiabatic and fast oscillation behavior). From this analysis we conclude that the adiabatic compression of matter wave solitons is possible in a wide range of the parameter s (i.e. $0 < s \approx 1$) and is compatible with relatively fast variations of the scattering length, as one can see from the top inset of Fig. 4.

4. Conclusions

In conclusion, we have shown that adiabatic changes of the scattering length, both in space and time, can be effectively used to control parameters of BEC matter waves of soliton type. In particular we showed the effect of pulse compression both on dark and bright solitons in presence and absence of a confining parabolic potential. The influence of the smoothness of the transition was also considered. We found that deviations from adiabatic predictions occur only for very large values of s , i.e. for almost step-like variations. This implies that the results of this paper are valid for generic smooth variations of the scattering length and therefore are expected to be found in real BEC matter waves experiments. The possibility of sharpening bright and dark solitons by means of smooth variations of the scattering length, beside providing another confirmation of the soliton nature of the BEC ground state, may be very useful for concrete applications. We hope that experiments in this direction will be soon performed.

Acknowledgments

We are grateful to V.V. Konotop for interesting discussions. F.Kh.A. acknowledges the hospitality received at the Physics Department of the University of Salerno, where this work was done, and partial financial support from NATO-Linkage grant No. PST.CLG.978177. M. S. thanks the European grant LOCNET no. HPRN-CT-1999-00163 for partial support.

References

- [1] Denschlag et al., *Science*, **287** (2000) 97.
- [2] Strecker K., Patridge G., Truscott A., and Hulet R., *Nature*, **417** (2002) 150.
- [3] Khaykovich L., et al., *Science*, **296** (2002) 1290.
- [4] Carr L.D. and Castin Y., *Phys.Rev. A*, **66** (2002) 063602.
- [5] Salerno M., Samuelsen M.R., Lomdahl P.S., and Olsen O.H., *Phys.Lett.*, **108A** (1985) 241; Pagano S., Salerno M., and Samuelsen M.R., *Physica D*, **26** (1987) 396.
- [6] Quiroga-Teixeiro M.L. et al., *JOSA B*, **13** (1996) 687.
- [7] Nistazakis H.E., et al., arXiv:cond-mat/0211702 v1.
- [8] Peréz-García V.M., Michinel H., Herrero H., *Phys.Rev. A*, **57** (1998) 3837.
- [9] Reinhardt W.P. and Clark C.W., *J.Phys.*, B, **30** (1997) L785.
- [10] Malomed B.A., In *"Progress in Optics"*, Ed.E. Wolf, **43**, 71, 2002.
- [11] Turitsyn S.K., *JETP Letters*, **65** (1997) 845.
- [12] Abdullaev F.Kh. and Caputo J.G., *Phys.Rev. E*, **58** (1998) 6637.
- [13] Salasnich L., Parola A., and Reatto L., *Phys.Rev. A* (2002) **043603**.
- [14] Karpman V.I., *Phys.Scripta*, **20** (1979) 462.
- [15] Zhao W. and Bourkoff E., *Opt.Lett*, **14** (1989) 703.
- [16] Abdullaev F.Kh., Nurmanov N., and Tsoy E.N., *Phys.Rev. E*, **56** (1997) 3638.